Validation of a High-Resolution Version of the Regional Climate Model RegCM3 over the Carpathian Basin

CSABA TORMA

Department of Meteorology, Eötvös Loránd University, and Adaptation to Climate Change Research Group, HAS-BCU, Budapest, Hungary

ERIKA COPPOLA AND FILIPPO GIORGI

Earth System Physics Section, Abdus Salam International Centre for Theoretical Physics, Trieste, Italy

JUDIT BARTHOLY AND RITA PONGRÁCZ

Department of Meteorology, Eötvös Loránd University, Budapest, Hungary

(Manuscript received 4 November 2009, in final form 21 August 2010)

ABSTRACT

This paper presents a validation study for a high-resolution version of the Regional Climate Model version 3 (RegCM3) over the Carpathian basin and its surroundings. The horizontal grid spacing of the model is 10 km—the highest reached by RegCM3. The ability of the model to capture temporal and spatial variability of temperature and precipitation over the region of interest is evaluated using metrics spanning a wide range of temporal (daily to climatology) and spatial (inner domain average to local) scales against different observational datasets. The simulated period is 1961–90. RegCM3 shows small temperature biases but a general overestimation of precipitation, especially in winter; although, this overestimate may be artificially enhanced by uncertainties in observations. The precipitation bias over the Hungarian territory, the authors' main area of interest, is mostly less than 20%. The model captures well the observed late twentieth-century decadal-to-interannual and interseasonal variability. On short time scales, simulated daily temperature and precipitation show a high correlation with observations, with a correlation coefficient of 0.9 for temperature and 0.6 for precipitation. Comparison with two Hungarian station time series shows that the model performance does not degrade when going to the 10-km gridpoint scale. Finally, the model reproduces the spatial distribution of dry and wet spells over the region. Overall, it is assessed that this high-resolution version of RegCM3 is of sufficiently good quality to perform climate change experiments over the Carpathian region—and, in particular, the Hungarian territory—for application to impact and adaptation studies.

1. Introduction

The Carpathian basin is surrounded by the Carpathians to the east, the Dinaric Mountains to the south and the Alps to the west (Fig. 1). Thus, the Carpathian basin region includes flat areas, such as the Hungarian lowlands along with complex topography (the Carpathians), and this varied morphological structure plays a major role in determining the climate of the basin. The dominant wind direction over the basin is west-northwest, resulting in a west-to-east spatial gradient of precipitation modulated by local topography. The annual average precipitation over Hungary is about 600–650 mm; however, the spatial distribution of precipitation is highly varied, from humid conditions in the southwestern part of the basin, where the effect of the Mediterranean Sea is considerable, to semiarid conditions over eastern Hungary.

Climate scenarios produced in support of the Fourth Assessment Report of the Intergovernmental Panel on Climate Change (Solomon et al. 2007) suggest changes in regional climate conditions during the twenty-first century, such as drier and hotter summers over central Europe. Moreover, studies with different greenhouse gas emission scenarios show that Europe is one of the earth's most sensitive regions to global warming (Giorgi 2006), and that the Carpathian basin is located in a

Corresponding author address: Csaba Torma, Eötvös Loránd University, P.O. Box 32, H-1518 Budapest, Hungary.
E-mail: delivitez@nimbus.elte.hu

DOI: 10.1175/2010JHM1234.1

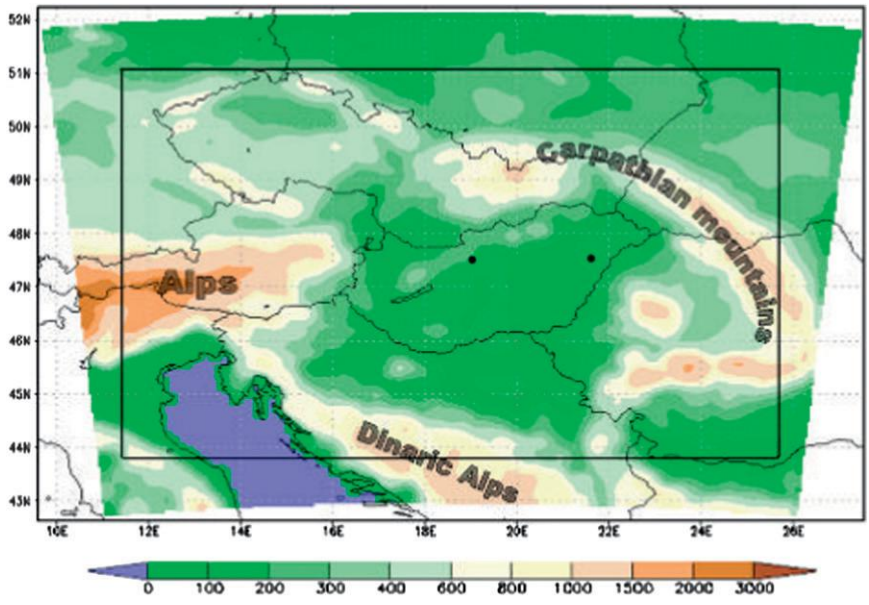

FIG. 1. Model domain and topography (m) at a grid spacing of 10 km. The box shows the interior domain (not directly affected by the lateral buffer zone and marked with black solid lines): 43.8°–51.045°N, 11.4°–25.75°E. The two dots show the location of the (left) Budapest and (right) Debrecen observing stations.

transition region of the precipitation change pattern (Giorgi and Coppola 2007). High-resolution climate model simulations are thus needed to provide accurate climate change scenarios accounting for this complex spatial and temporal modulation of the climate change signal.

Since most global coupled climate models are still run at horizontal resolutions of one to a few hundred kilometers, they cannot accurately describe the effects of the Carpathians and Alps mountain chains, and one technique that can be used to obtain climate change information at finer scales is the use of nested regional climate models (RCMs; Giorgi and Mearns 1999). An ensemble of RCM climate change simulations was recently produced as part of the Prediction of Regional Scenarios and Uncertainties for Defining European Climate Change Risks and Effects (PRUDENCE) project (Christensen and Christensen 2007; Jacob et al. 2007; Déqué et al. 2007). The grid spacing of the PRUDENCE RCMs, however, was about 50 km and, although higher than that of global models, was still not fully adequate to provide sufficiently detailed information for use in impact studies over the Carpathian basin.

The project Central and Eastern Europe Climate Change Impact and Vulnerability Assessment (CECILIA; Halenka 2007) was thus developed to produce higher-resolution simulations over different subregions of central Europe, including the Carpathian basin. Different RCMs were run for this purpose at a grid spacing of 10 km, a resolution that represents the limits of application of the hydrostatic RCMs, such as the one used here. This requires the models to be carefully tested and optimized before the climate change simulations are carried out.

In this paper we present a validation analysis of a recent past climate simulation over the Carpathian basin with the Abdus Salam International Centre for Theoretical Physics (ICTP) RegCM3, one of the CECILIA high-resolution RCMs. As mentioned, the model is run at 10-km grid spacing, which is to date the highest resolution reached by the RegCM3 in climate simulations. Previous high-resolution simulations with RegCM (20-km grid spacing) include those of Marinucci et al. (1995) over the alpine region and Gao et al. (2006) over the full Mediterranean Basin. Some modifications were implemented to the standard version of RegCM3 as discussed by Torma et al. (2008), consisting mostly of changes of some parameters in the precipitation scheme aimed at removing some marked temperature and precipitation biases revealed by preliminary tests.

The simulation analyzed here covers the 30-yr period of 1961–90 over a domain encompassing Hungary (our main region of interest) and the entire Carpathian basin. The boundary conditions for the model simulation are obtained from the 40-yr European Centre for Medium-Range Weather Forecasts Re-Analysis (ERA-40) dataset of observations, and different statistics of simulated temperature and precipitation covering a range of spatial and temporal scales are validated against gridded datasets and a limited number of station observations.

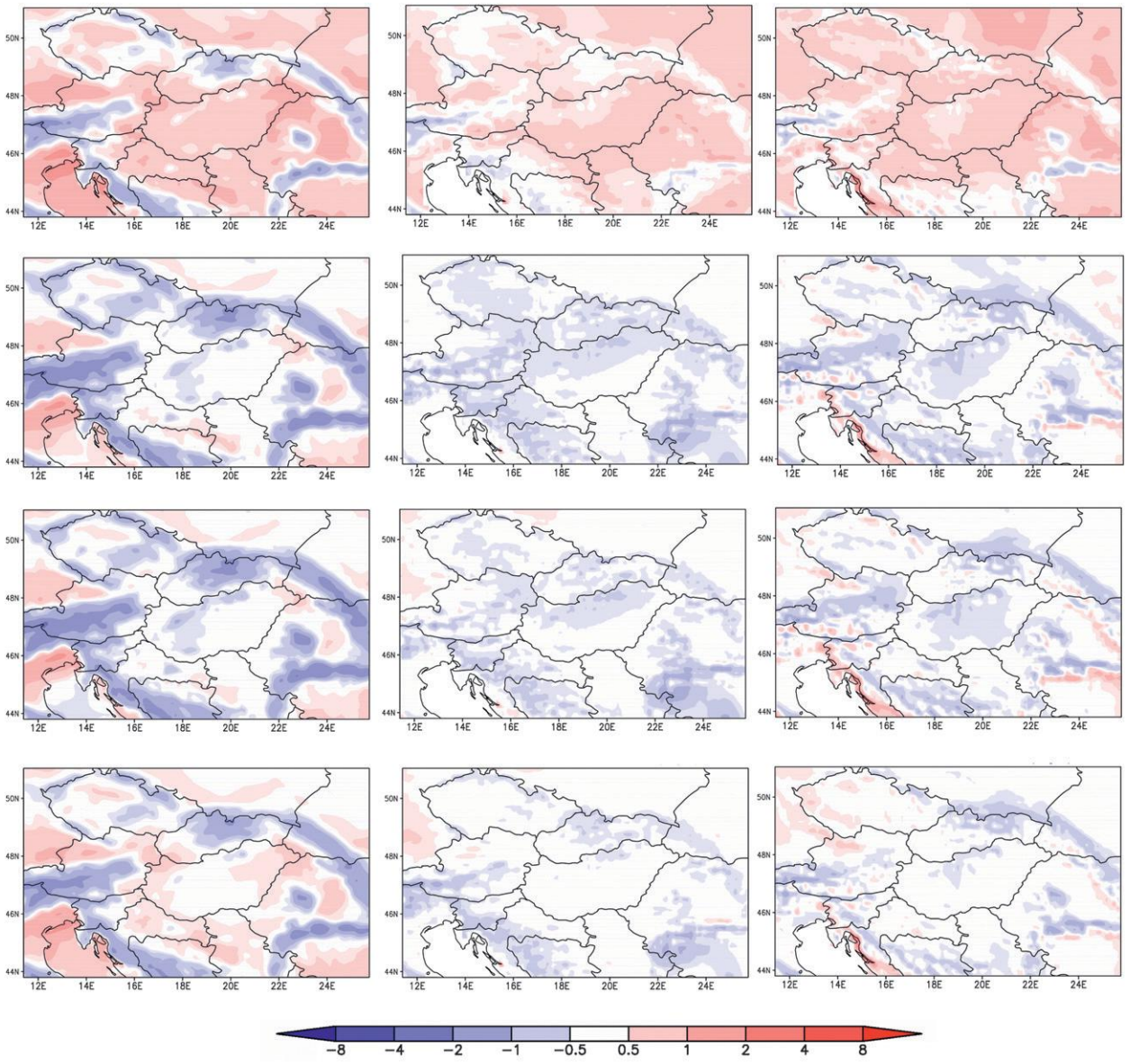

FIG. 2. Mean surface air temperature (°C) biases (1961–90) for (top to bottom) DJF, March–May (MAM), June–August (JJA), and September–November (SON) compared to (left) ERA-40 and (middle) E-OBS, and (right) compared to CRU TS1.2.

2. Model description

The RegCM3 version used here was originally developed by Giorgi et al. (1993a,b) and later modified and improved as described by Giorgi and Mearns (1999) and Pal et al. (2007). It is a hydrostatic and terrain-following sigma vertical coordinate model, whose dynamical core is essentially the same as that of the hydrostatic version of the fifth-generation Pennsylvania State University–National Center for Atmospheric Research (NCAR) Mesoscale Model (MM5; Grell et al. 1994). The Biosphere–Atmosphere Transfer Scheme (BATS; Dickinson et al. 1993) is used to represent surface processes, while boundary layer physics is described via the nonlocal vertical diffusion scheme of Holtslag et al. (1990). Other physics parameterization schemes include the radiative transfer package of the NCAR Community Climate Model version 3 (CCM3; Kiehl et al. 1996), the mass flux cumulus cloud scheme of Grell (1993) to represent convective precipitation, and the resolvable-scale precipitation scheme of Pal et al. (2000), which includes a prognostic equation for cloud water and allows the determination of subgrid-scale cloud fraction. (The standard version of the model is available online at http://users.ictp.it/~pubregcm/RegCM3/.)

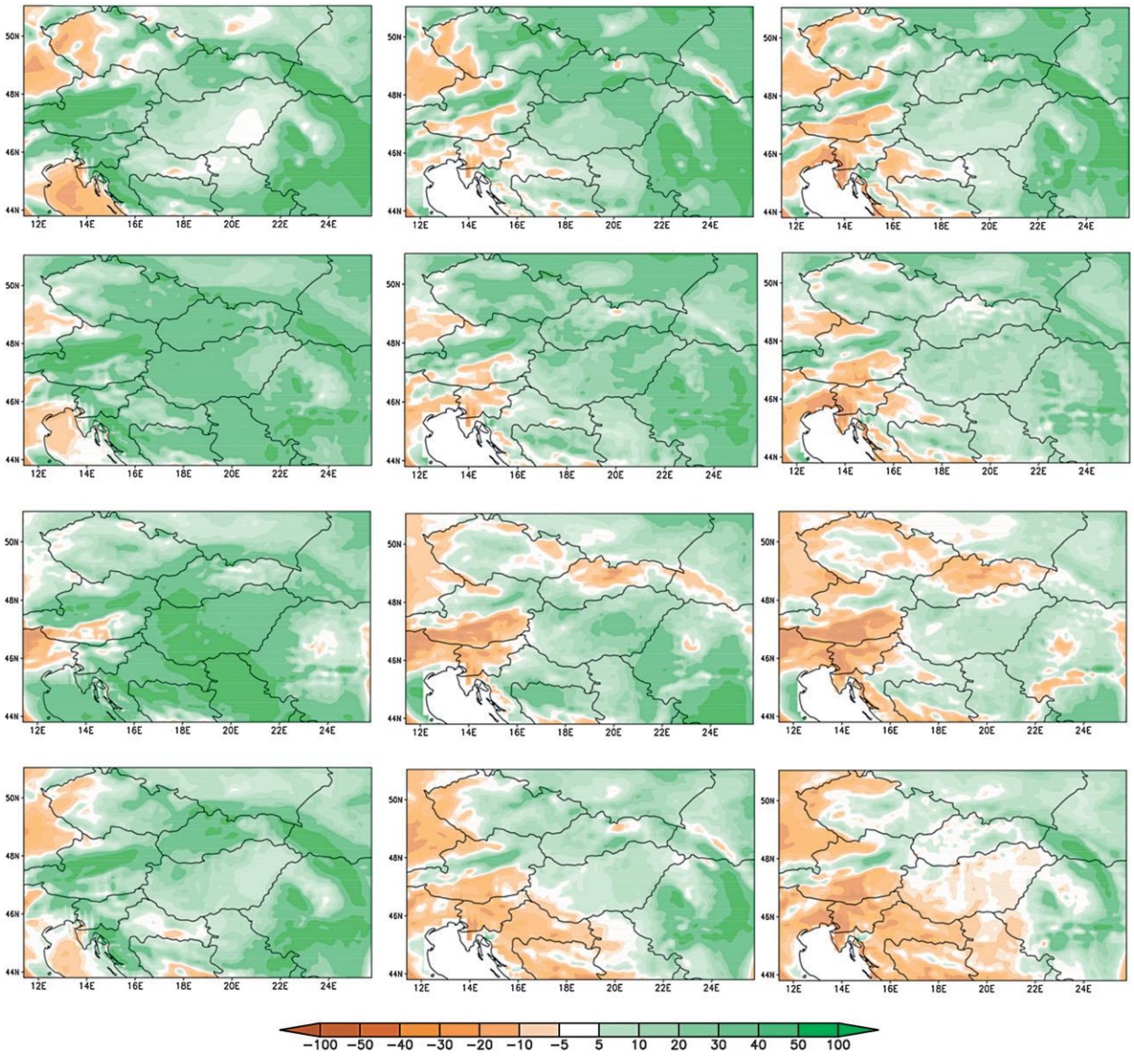

FIG. 3. As in Fig. 2, but for precipitation (mm day^{-1}).

A number of model tests were conducted to evaluate the performance of different convection schemes and parameter setups for the model domain and to reduce precipitation and temperature biases found in preliminary experiments (Torma et al. 2008). According to such tests, the standard version RegCM3 substantially overestimated precipitation over the whole domain, except for the southeastern portions of the Alps. To decrease precipitation, the following three parameters were modified in the resolvable precipitation scheme: the cloud-to-rain autoconversion rate was decreased from 0.0005 to 0.00025, the raindrop evaporation rate coefficient was increased from 0.2×10^{-4} to 1.0×10^{-3} (kg m^{-2} s^{-1})$^{-1/2}$ s^{-1}, and the raindrop accretion rate was decreased from 6 to 3 m^3 kg^{-1} s^{-1}. Further discussion and details of the evaluation of the standard and modified RegCM3 experiments are in Torma et al. (2008).

3. Experiment design and observation datasets

The integration domain includes the Carpathian basin and surrounding areas at 10-km grid spacing and 18 vertical sigma levels. The model domain and topography are shown in Fig. 1. The domain is 120 × 100 grid points in the horizontal and meridional directions, respectively, while the lateral buffer zone is 12 grid points at all

TABLE 1. Observed and simulated interior domain average of gridpoint interannual variability for seasonal temperature and precipitation. The interannual variability is measured by the interannual standard deviation for temperature (°C) and the interannual coefficient of variation (standard deviation divided by the mean, unitless) for precipitation.

	ERA-40	E-OBS	CRU	RegCM3	ERA-40	E-OBS	CRU	RegCM3
	IAV of temperature				IAV of precipitation			
DJF	2.9	3.1	3.1	2.3	0.48	0.58	0.52	0.51
MAM	1.4	1.5	1.5	1.5	0.4	0.44	0.41	0.48
JJA	1.4	1.4	1.4	1.4	0.49	0.46	0.41	0.46
SON	1.4	1.5	1.4	1.5	0.65	0.72	0.62	0.68

boundaries. The main topographical features of the interest region—such as the Carpathians to the east, the Alps to the west, the Dinaric Mountains to the south, and a small fraction of the Adriatic Sea—are represented. The simulation period is 1961–90, and the lateral meteorological boundary conditions necessary to run the model are obtained from the ERA-40 dataset of observations (Uppala et al. 2005) with a grid spacing of 2.5° × 2.5°. Our analysis focuses on temperature and precipitation, and for the model validation we use the gridded observation dataset produced as part of the Ensembles-Based Predictions of Climate Changes and Their Impacts (ENSEMBLES) project, E-OBS version 1.0 (referred to as the E-OBS dataset; Haylock et al. 2008). The E-OBS dataset is available on a ¼° grid (about 25 km) for the full simulation period, and it includes daily values of temperature and precipitation. We interpolate the E-OBS data onto the RegCM3 grid using a bilinear interpolation. The RegCM3 model results are also compared with the driving ERA-40 dataset

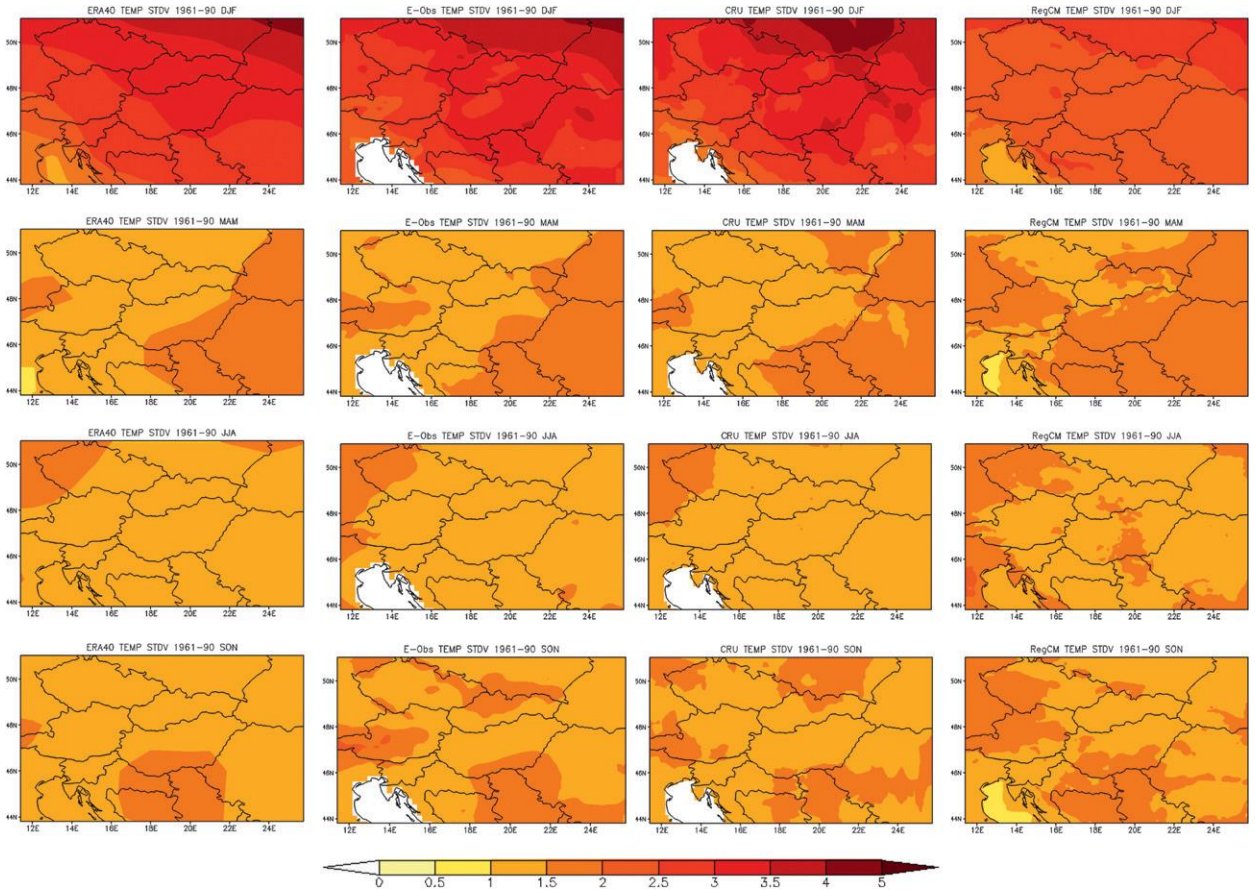

FIG. 4. Seasonal temperature (°C) interannual standard deviation for the period 1961–90 in the (first column) ERA-40, (second column) E-OBS observations, (third column) CRU, and (fourth column) RegCM3 simulation.

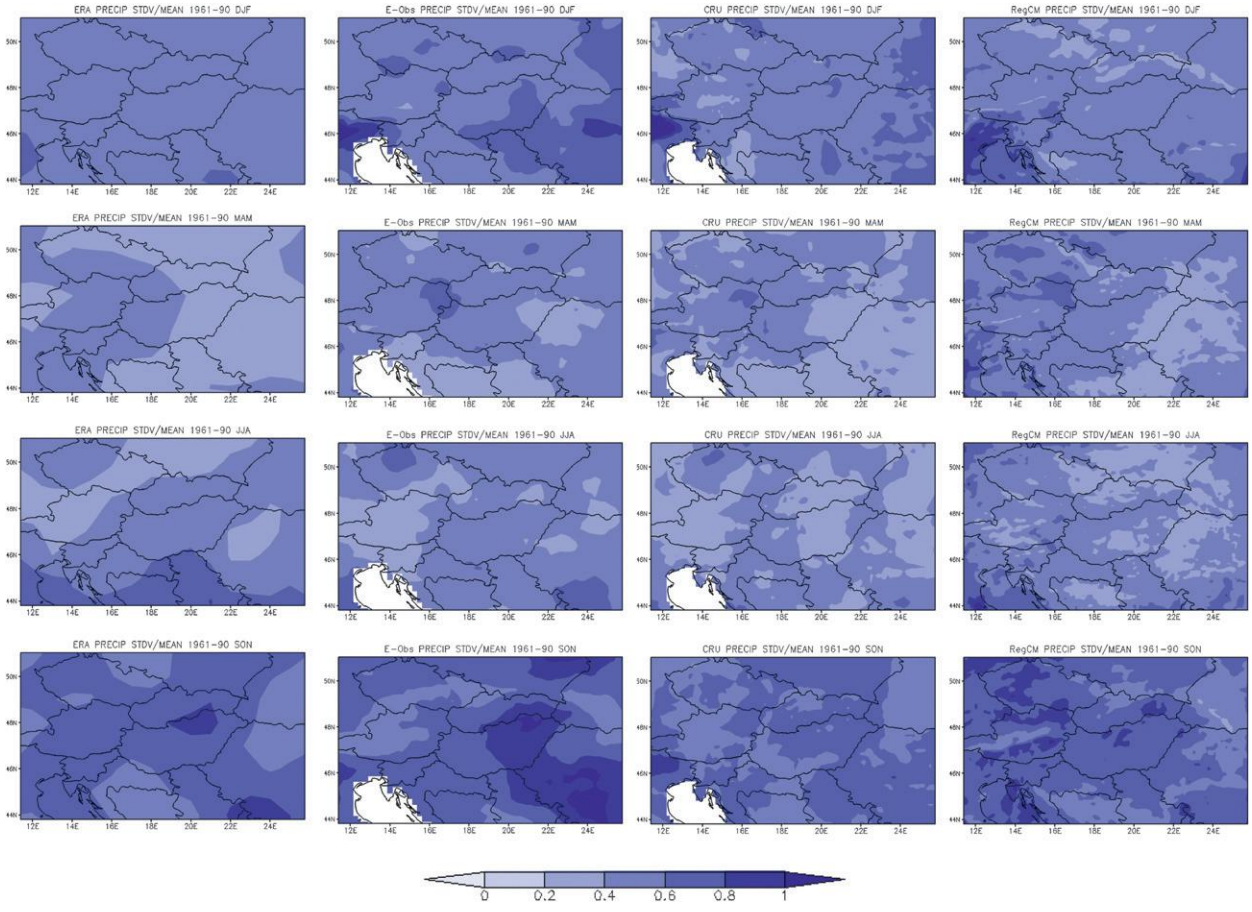

FIG. 5. As in Fig. 4, but for seasonal precipitation interannual coefficient of variation (unitless).

(Uppala et al. 2005) and the Climatic Research Unit (CRU) TS 1.2 dataset (referred to as CRU; Mitchell et al. 2004) interpolated onto the model grid.

To evaluate the model at the local scale, we present an additional validation of monthly-mean temperature and precipitation against observed data provided by the Hungarian Meteorological Service (HMS) for the period 1961–90. For this exercise we use data for two stations, Budapest (47.5°N, 19°E) and Debrecen (47.5°N, 21.6°E), that have continuous data for the entire reference period 1961–90 (see Fig. 1). Budapest, the capital of Hungary, lies at around 100–200 m above sea level in the north-central area of the country. It is surrounded by small mountains to the west and to the north and has a temperate climate, with an average temperature of −1.6°C in January and 20.8°C in July. The annual average precipitation in Budapest is approximately 507 mm, with a maximum in June (63 mm) and a minimum in March (29 mm). Debrecen is the second largest city in Hungary. It is located at about 100 m above sea level and lies in the Hungarian open Great Plain, close to the Romanian border. At Debrecen the average temperature varies between −2.6°C in January and 20.3°C in July, while the total annual precipitation is 566 mm, with a minimum in February (30 mm) and a maximum in June (80 mm). The station data are compared with those from the nearest model grid point, whose elevation at both locations is less than 25 m from that of the reporting station, indicating that elevation differences between model gridpoint and station locations is not an important factor in this comparison.

Finally, we note that all the observed datasets used in the model validation do not include any gauge undercatch correction, which can contribute up to 20%–30% of the total precipitation, especially for wintertime over mountainous areas (Adam and Lettenmaier 2003).

4. Results

Given the relatively small size of the domain, we do not expect that the model will substantially modify the basic features of the synoptic systems entering the domain. For example, we compared mean and variance of the 500-hPa geopotential height in the ERA-40

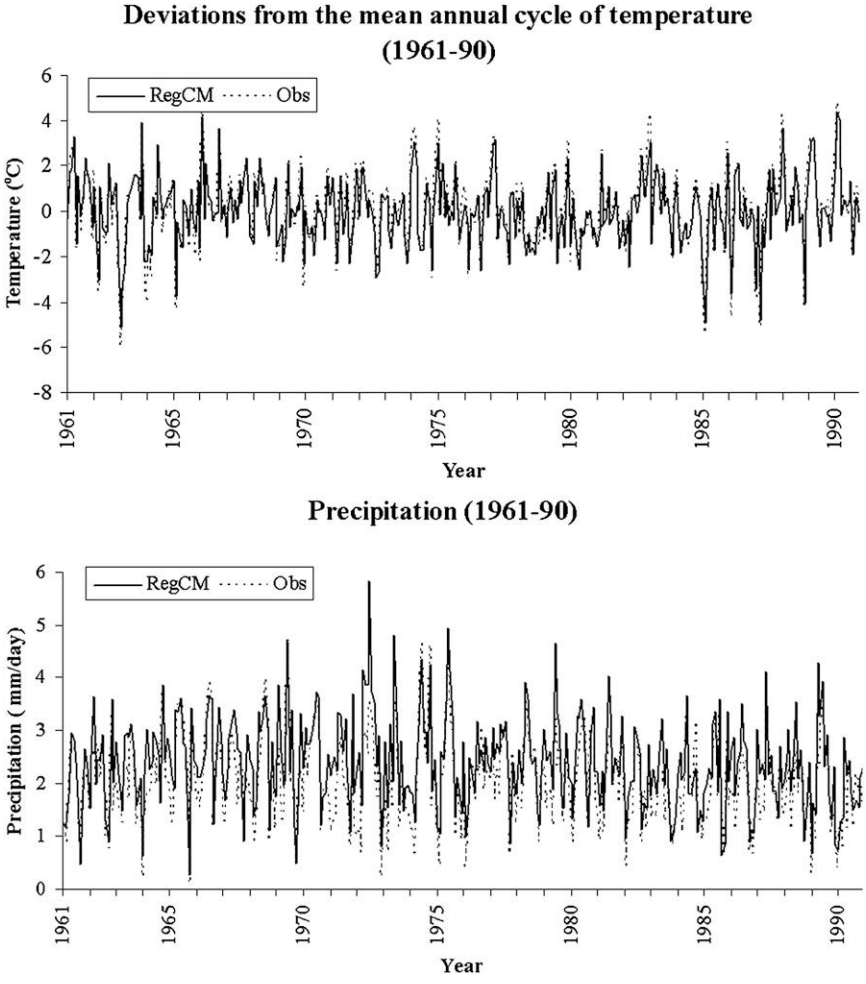

FIG. 6. Simulated monthly area-average (top) temperature anomaly (°C) and (bottom) monthly anomaly precipitation (mm day^{-1}) for the RegCM simulation and the E-OBS observations, respectively. The average is taken over the interior domain (see Fig. 1).

and RegCM3 and found only small differences not characterized by any systematic structure (not shown for brevity). Rather, our analysis focuses on how the model simulates surface climate (temperature and precipitation) in response to the large-scale forcing imposed by the ERA-40 reanalysis and by local topographical features.

a. Mean and interannual variability

In this section we first validate mean climate and interannual variability. All the analysis presented here is carried out over the interior domain shown in Fig. 1 to eliminate the buffer zone where the direct effect of the lateral boundary conditions is maximum. Figures 2 and 3 show the spatial distribution of seasonal temperature and precipitation biases averaged over the entire 30-yr period compared to the ERA-40, E-OBS, and CRU datasets.

In all seasons the temperature bias against E-OBS and CRU data ranges between −1° and 1°C over most of the domain, except in winter when the bias mostly ranges between 0° and 2°C. Differences between RegCM3 and ERA-40 data range between −4° and 4°C, and we notice from the spatial distribution of these differences that the maximum values occur over the mountainous areas. This is a clear effect of the different resolutions in the datasets. For all three observation datasets, a prevailing warm bias is found in winter and a cold bias in spring, summer, and fall. Interior domain-average biases are 0.8° in winter, −0.5° in spring, −0.4° in summer, and −0.3°C in autumn when E-OBS is considered, while they are slightly smaller when the CRU dataset is used (1.0° winter, −0.4° spring, −0.3° summer, and −0.2°C autumn) and larger when compared to the ERA-40 dataset (0.8° winter, −0.7° spring, −0.8° summer, and −0.2°C autumn). These negative temperature biases are smaller than those obtained by Csima and Horányi (2008) in a similar simulation over the same region

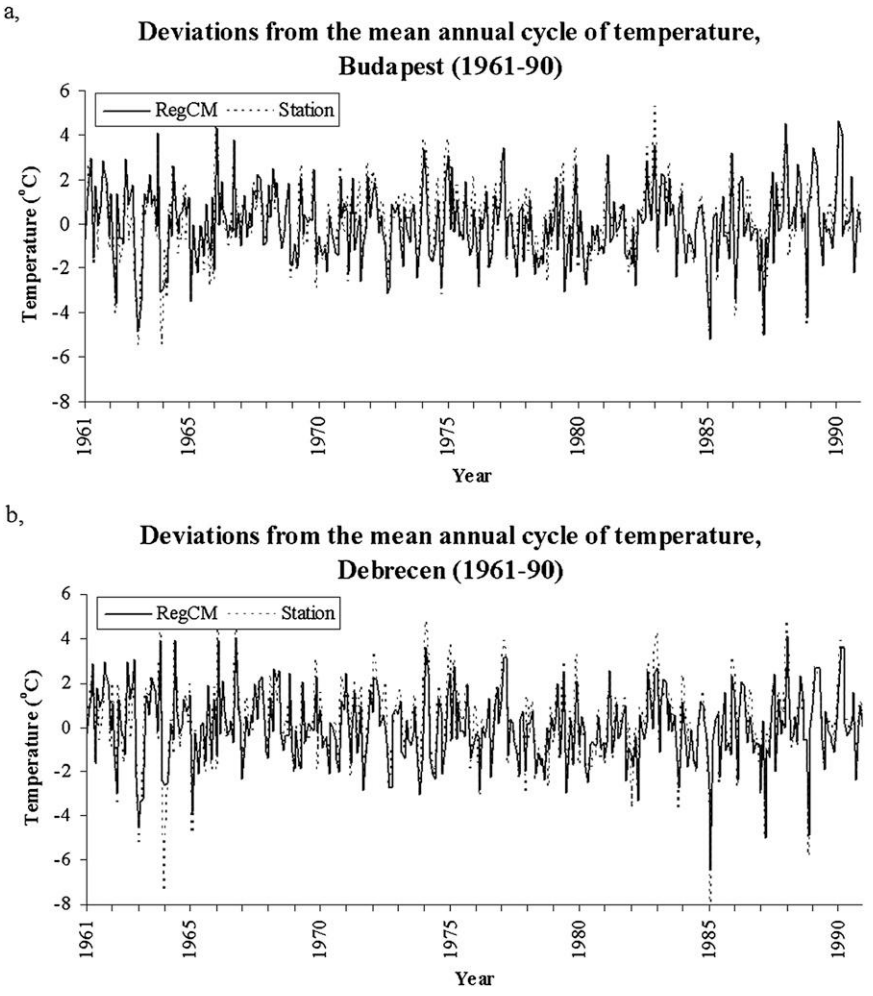

FIG. 7. Simulated (solid line) and observed (dotted line) monthly-mean temperature (°C) anomalies at (a) Budapest and (b) Debrecen (see Fig. 1). The datasets cover the period 1961–90.

with a different RCM. The largest biases compared to E-OBS (about 2°C) are found over the eastern part of the Carpathian basin, and a systematic cold bias is found over the mountainous areas of the alpine region and the coastal Balkans. The latter, however, is probably amplified by the relative lack of high-elevation-observing stations in mountainous regions and the lack of a topographic correction in the station dataset. Autumn is the season for which temperature is best simulated, with small biases throughout most of the domain. Overall, the bias values found in this simulation are small compared to previous experiments for this area, with RegCM3 operating on a 20-km resolution (Gao et al. 2006), and are within the range expected of state-of-the-art RCMs (Giorgi and Mearns 1999).

Seasonal precipitation bias fields for 1961–90 are shown in Fig. 3. For the interior domain average, an overestimation of precipitation is found in all seasons compared to E-OBS, about 49% in winter, 40% in spring, 23% in summer, and 16% in autumn. Compared to the CRU dataset, the overestimation decreases in all seasons (35% winter, 25% spring, 5% summer, and 3% autumn), and in autumn a negative bias is found in the central and southwestern portions of the domain. Figure 3 shows that precipitation is generally underestimated in the western portions of the domain, close to the ''entrance'' boundary of the prevailing eastward-moving storms. This may indicate that these regions are still affected by the lateral boundary conditions even if they are outside the boundary zone. The largest positive biases are found over the Carpathian chain in the colder seasons. As noted above, however, this large bias may be artificially enhanced by the lack of an undercatch correction in the observations (Adam and Lettenmaier 2003), which can reach up to 20%–30% in winter. Moreover, these biases are comparable to, or smaller than,

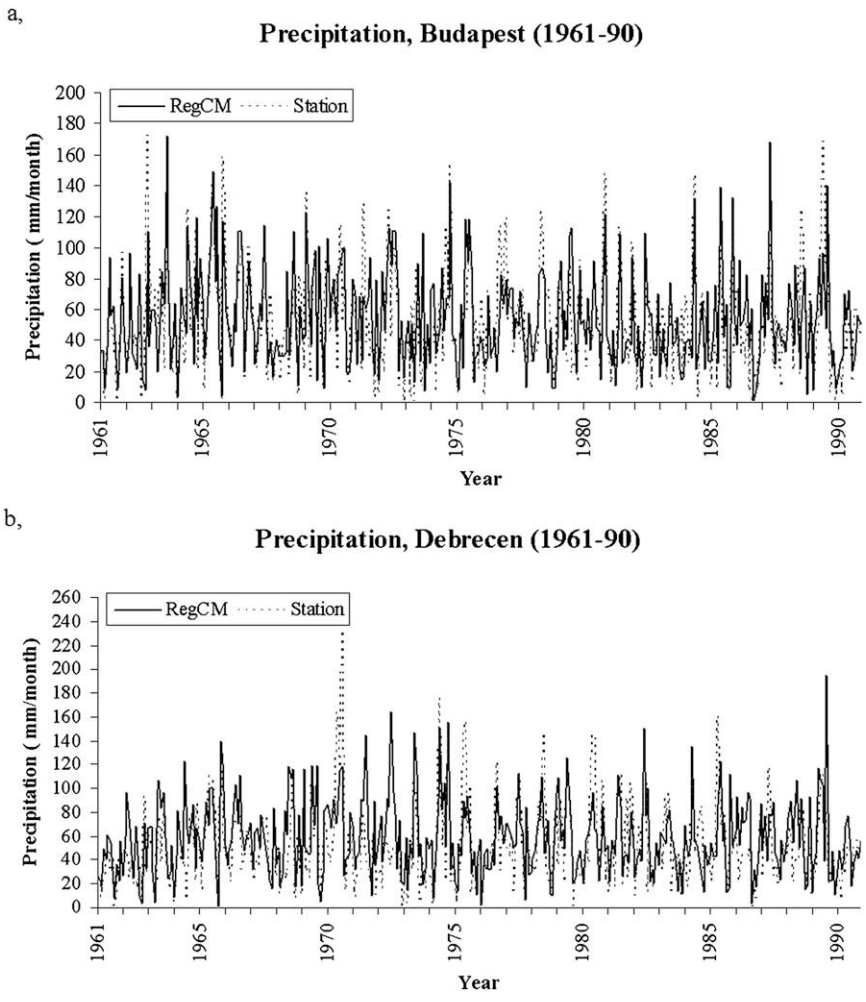

FIG. 8. Simulated (solid line) and observed (dotted line) total monthly precipitation (mm month^{-1}) at (a) Budapest and (b) Debrecen.

those found by Csima and Horányi (2008), where for all seasons except winter the overestimation of precipitation is more pronounced.

The comparison of the model data with the ERA-40 precipitation shows that the RegCM3 has higher precipitation almost everywhere in the domain (47% winter, 54% spring, 52% summer, and 42% autumn), with differences greater than those found with respect to E-OBS and CRU. This means that ERA-40 is underestimating precipitation throughout the domain compared to the observed datasets. Focusing on the innermost portion of the domain covering the Hungarian territory (our main area of interest), the bias compared to E-OBS is about 20% or less in all seasons and even lower when CRU is considered. These values are within the range typically found in state-of-the-art RCMs (Giorgi and Mearns 1999).

Simulated interannual variability (IAV) of temperature and precipitation is computed and compared with the IAV of the ERA-40, E-OBS, and CRU seasonal data for the 30-yr reference period 1961–90. The IAV is measured by the interannual standard deviation for temperature and the coefficient of variation (standard deviation divided by the mean; Räisänen 2002) for precipitation. Table 1 reports the interannual variability of simulated and observed (ERA-40, E-OBS, and CRU) temperatures averaged over the interior domain (see Fig. 1). The model reproduces the seasonal distribution of IAV, with a maximum in winter. The largest difference between simulated and observed temperature IAV occurs in winter, when the model IAV is lower than observed by about 0.6°C compared to ERA-40 and 0.8°C compared to E-OBS and CRU. In the other seasons, the errors in IAV are small, less than a tenth of a degree.

Figure 4 shows the spatial distribution of the simulated and observed temperature IAV. The model reproduces well the general spatial distribution of temperature IAV

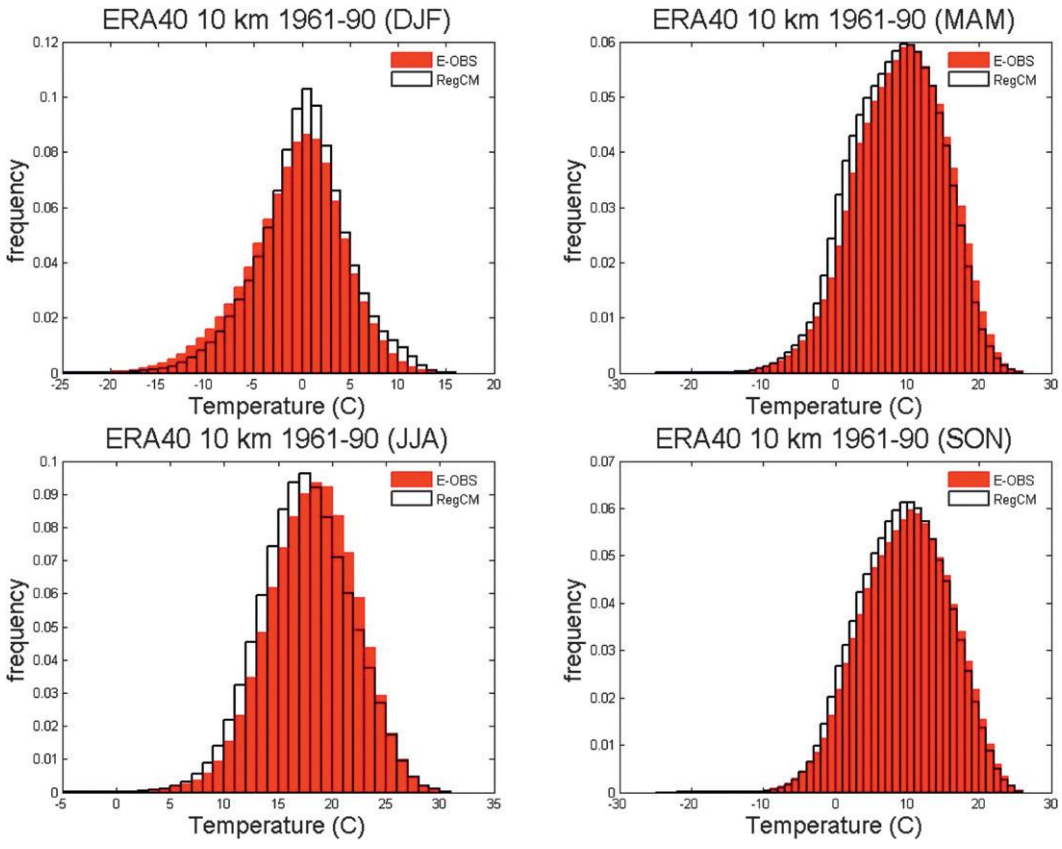

FIG. 9. Simulated (black solid) and observed (red) gridpoint daily temperature distributions for the four seasons. The figure accounts for all grid points in the interior domain.

in all seasons. The agreement with observations is best in autumn, both in terms of magnitude and spatial distribution. The IAV of temperature in spring and summer is also close to observations, although the model shows excessively high values over the lowlands in the center of the domain. In winter the model reproduces the northward gradient of IAV, but it underestimates the IAV particularly in the central portions of the domain.

The IAV of precipitation (as measured by the coefficient of variation) shows a substantial spatial variability, which is illustrated by the maps in Fig. 5. In general, the model shows more pronounced spatial variability of precipitation IAV than observed in the western part of the domain, probably because of the coarser resolution of the observed data and also because of the uncertainty of the interpolation error in the observed dataset as reported in Hofstra et al. (2009). The model captures the general magnitude of the observed precipitation IAV (see also Table 1). In spring and summer, the model reproduces the spatial patterns of IAV, for example, the spring maximum over eastern Austria. The magnitude of IAV is in line with observations (see Table 1), but some regional patterns are not well reproduced (i.e., in winter over the eastern chains of the Carpathians and in autumn over the southeastern chains of the Carpathians and over the northwestern region of the Czech Republic). As with temperature, the model generally reproduces the seasonal evolution of IAV, with a marked autumn maximum.

Figure 6 shows the inner domain area-average temperature deviations from the mean annual temperature cycle and the monthly evolution of precipitation for the model and observations. A high correlation between the simulated and observed time series (0.97) shows that the model reproduces well the observed temperature deviations from the mean annual cycle. The largest differences occur in winter (i.e., almost 2.5°C in January 1964). Also reproduced is the decadal temperature variability, for example, with a maximum in the mid-1970s and late 1980s. Monthly precipitation is also well reproduced, with a correlation coefficient of 0.87. The model positive precipitation bias mentioned above is evident from Fig. 6, as is the good model performance in reproducing the observed interannual and intraseasonal variability.

Moving to the local scale, Figs. 7 and 8 show the simulated and observed monthly deviation of temperature and

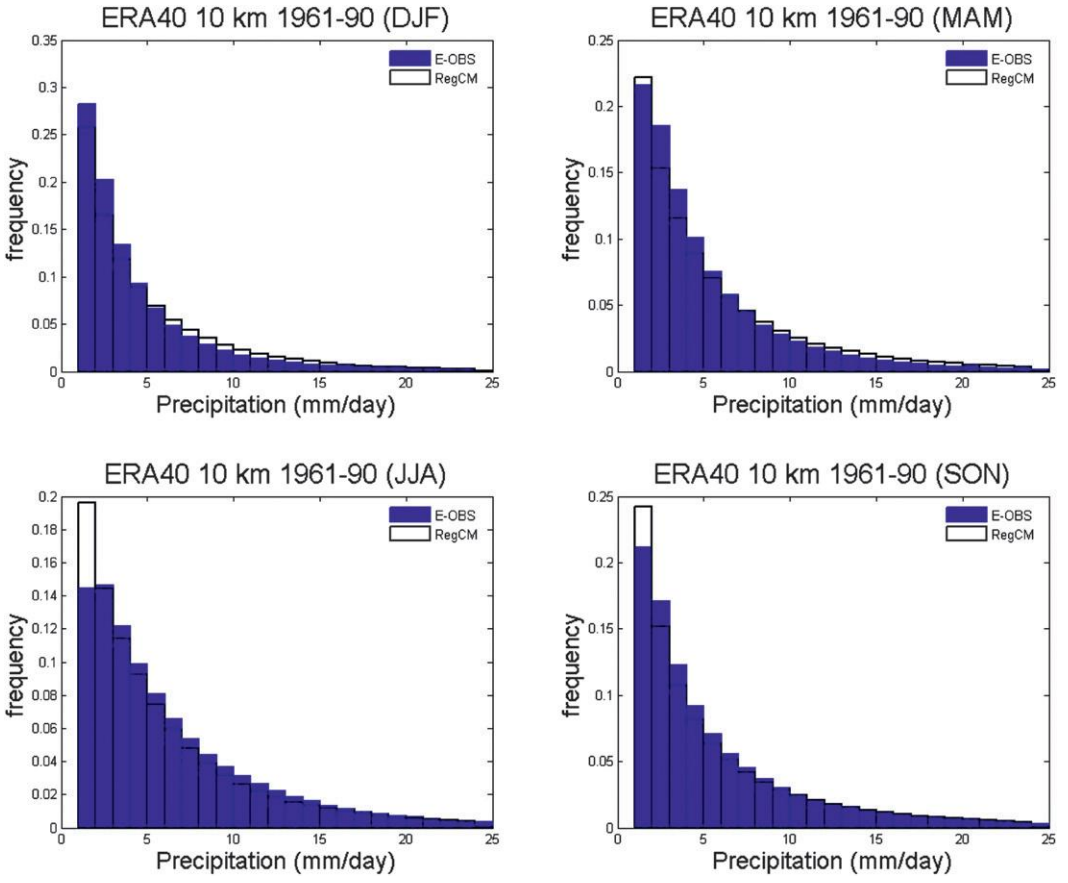

FIG. 10. As in Fig. 9, but for precipitation. The blue bars indicate the E-OBS, and the PDFs are normalized by the corresponding total number of rainy events.

the monthly-mean precipitation time series, respectively. For temperature, the average bias over the whole period is about −1.1°C at Budapest and 0.5°C at Debrecen. For Budapest, most of the cold bias occurs in the peak summer months, while at Debrecen the model tends to overestimate minimum winter temperatures. In both cases the model reproduces well both the seasonal cycle and the interdecadal variability. In fact, for the entire period the correlation coefficient between simulated and observed monthly temperatures is close to 0.93 at both stations. For precipitation, the model performs better at Budapest than at Debrecen. At Budapest, the average bias for the period 1961–90 is about 0.24 mm day^{-1}, with a correlation coefficient between simulated and observed monthly precipitation of 0.71. At Debrecen the bias is 0.37 mm day^{-1} and the correlation coefficient is 0.63. The bias is positive in all seasons except autumn. In both cases the model's interannual and intraseasonal variability is in line with observations. Overall, although limited to two stations, the analysis presented here indicates that the model performance does not deteriorate substantially when we move to the local scale.

b. *Daily temperature and precipitation*

After having examined the long-term climatology and the interannual and intraseasonal time scales, in this section we turn our attention to the daily time scale. Toward this purpose we use the E-OBS 25-km daily observed data. Figure 9 first shows simulated and observed daily temperature distributions, including all grid points in the interior domain. The model closely reproduces the observed distributions in spring and fall. In winter the simulated distribution is somewhat more peaked and displaced toward higher temperatures than observed, while in summer a slight shift toward lower temperatures is found. The width of the distribution is generally consistent between model and observations in all seasons.

Figure 10 presents the simulated and observed grid point normalized daily precipitation distributions, including all grid points in the interior domain and days with more than 1 mm of precipitation (i.e., "wet days"; Sansom and Renwick 2007). In all seasons except winter, the model overestimates the frequency of occurrence of

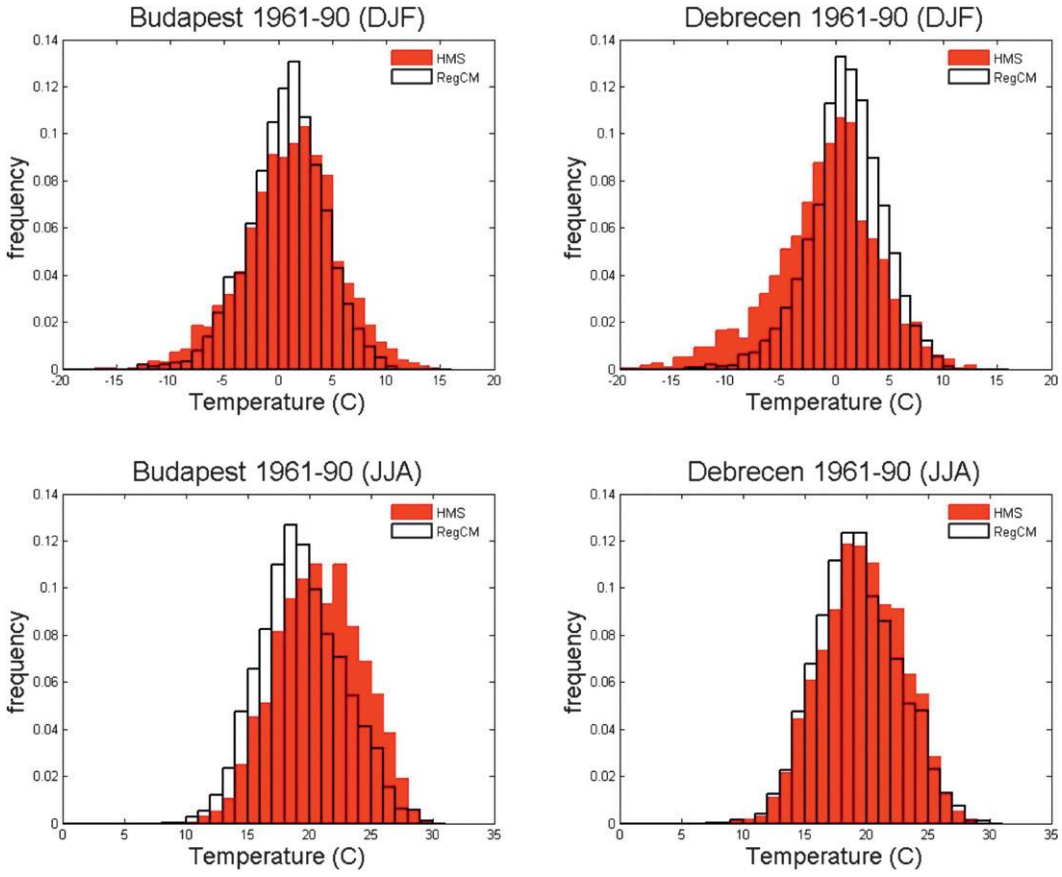

FIG. 11. Simulated (black solid) and observed (red) gridpoint daily temperature distributions for (top) DJF and (bottom) JJA at (left) Budapest and (right) Debrecen.

the lightest precipitation category events (<2 mm day^{-1}). In December–February (DJF), the frequency of light precipitation events (<5 mm day^{-1}) is underestimated and that of higher precipitation events is slightly overestimated, while the opposite occurs in summer. Some small differences between observed and simulated normalized frequencies are found in spring and autumn for events <10 mm day^{-1}, with good agreement for more intense events. Of relevance in Fig. 10 is that the heavy precipitation tail appears well simulated in all seasons.

At the two Hungarian stations, the simulated and observed daily temperature and precipitation probability density functions (PDFs) (Figs. 11 and 12) show an agreement consistent with that found for the overall interior domain, except in winter. More specifically, the winter temperature PDF at the Budapest station (Fig. 11) shows a shape similar to that of the whole domain (Fig. 9), while at Debrecen (Fig. 12) the model distribution is more peaked and shifted toward warmer events. We calculated some quantitative measures of differences between the simulated and observed PDFs, such as the 5th and 95th percentiles (see Table 2) and found differences of less than 1.5°C, except for the 5th percentile in DJF at Debrecen (difference of about 5°).

The normalized daily precipitation PDFs generally show good agreement with observations (Fig. 12). The winter daily precipitation distribution at Debrecen is similar to the whole domain distribution, while the simulated distribution at Budapest shows some overestimation of the medium–light precipitation events (<5 mm day^{-1}). In summer the model shows an overestimation of the medium–high precipitation events (<10 mm day^{-1}) at both stations, which is not found for the whole domain distributions, and an underestimation of extreme events. In fact, the 5th percentiles are in line with observations (see Table 2), while the 95th percentiles are underestimated at both stations, especially in summer.

c. *Dry and wet spells*

In this section we present an assessment of the model's ability to reproduce dry and wet spell frequencies over the integration domain. In fact, the length of dry and wet periods is a key issue for agriculture and health. For

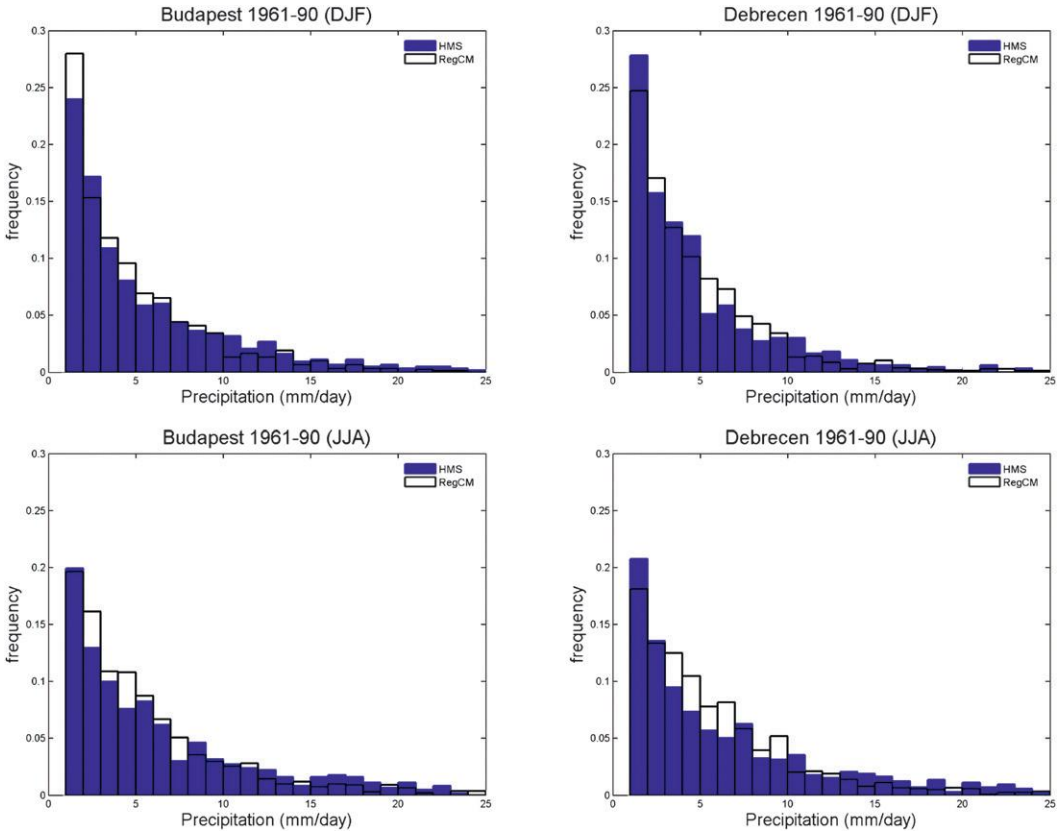

FIG. 12. As in Fig. 10, but for precipitation. The blue bars indicate the measurements (HMS) and the PDFs are normalized by the corresponding total number of rainy events.

example, precipitation in Hungary is an important limiting factor in agriculture, and the soil moisture content has a strong relationship with dry and wet spells. At the same time, wet spells influence different diseases for cereals, since, for example, saturated soils, high temperature, and high relative humidity can create favorable conditions for fungal diseases (Pardo et al. 2005).

Figures 13 and 14 show simulated and observed dry and wet spell frequencies, respectively. Here a dry spell is identified by a sequence of at least five consecutive days, with daily precipitation of less than 1 mm, while a wet spell is a sequence of at least five consecutive days with precipitation of more than 1 mm day^{-1}. Overall, the frequency of dry spells shows a seasonal evolution with a maximum in the fall and a minimum in the summer. The model reproduces this feature. Substantial spatial variability in the dry spell frequency is observed, with a minimum over the Alps and the Carpathian mountain chain and a pronounced maximum over the Hungarian lowlands. The model reproduces this feature quite well, while subregional differences between observed and simulated values can be found in each season. Figure 13 indicates that the model reproduces the main characteristics of dry spell occurrence over the simulation domain, particularly over the Hungarian territory, except for summer, when the model is underestimating the dry spell length.

Similarly, the model reproduces the seasonal evolution of wet spells (Fig. 14), with an overall maximum in spring and summer and a minimum in autumn, although

TABLE 2. Temperature (°C) and precipitation (mm day^{-1}) 5th and 95th percentiles at Budapest and Debrecen (DJF and JJA) in the station observation and model simulation datasets.

	Budapest				Debrecen			
	OBS		RegCM3		OBS		RegCM3	
Temperature	5%	95%	5%	95%	5%	95%	5%	95%
DJF	−6.5	7.7	−5.2	6.3	−10	6.4	−4.9	6.5
JJA	15.2	26.3	14.1	25.3	14.2	24.9	14.3	24.9
	Budapest				Debrecen			
	OBS		RegCM3		OBS		RegCM3	
Precipitation	5%	95%	5%	95%	5%	95%	5%	95%
DJF	1.2	16.9	1.1	13	1.1	12.8	1.1	11
JJA	1.1	24.9	1.2	16.9	1.1	28.3	1.2	16

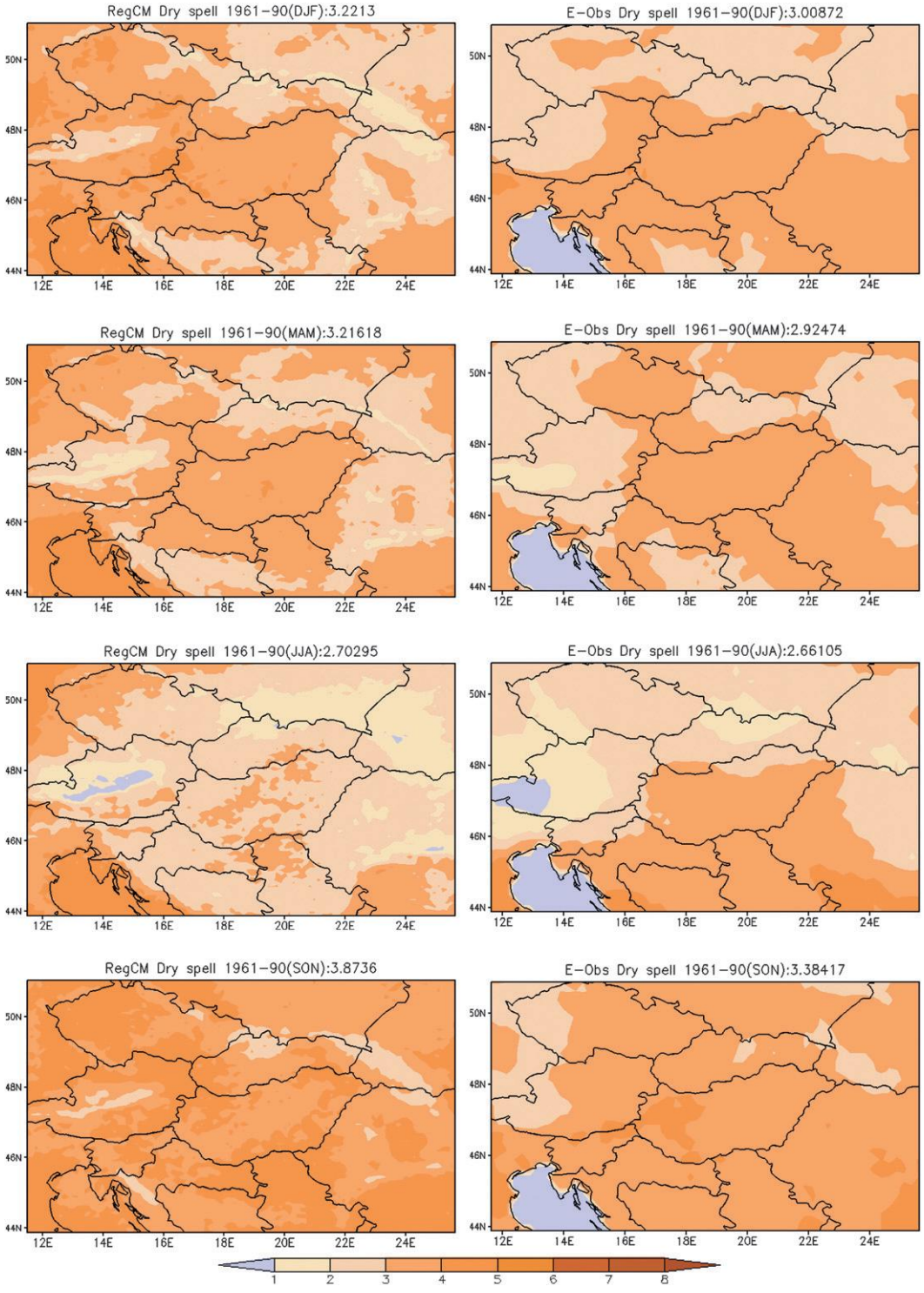

FIG. 13. Seasonal dry spell frequency (refer to text) through the period 1961–90 in the (left) RegCM3 simulation and (right) E-OBS observations for (top to bottom) DJF to SON.

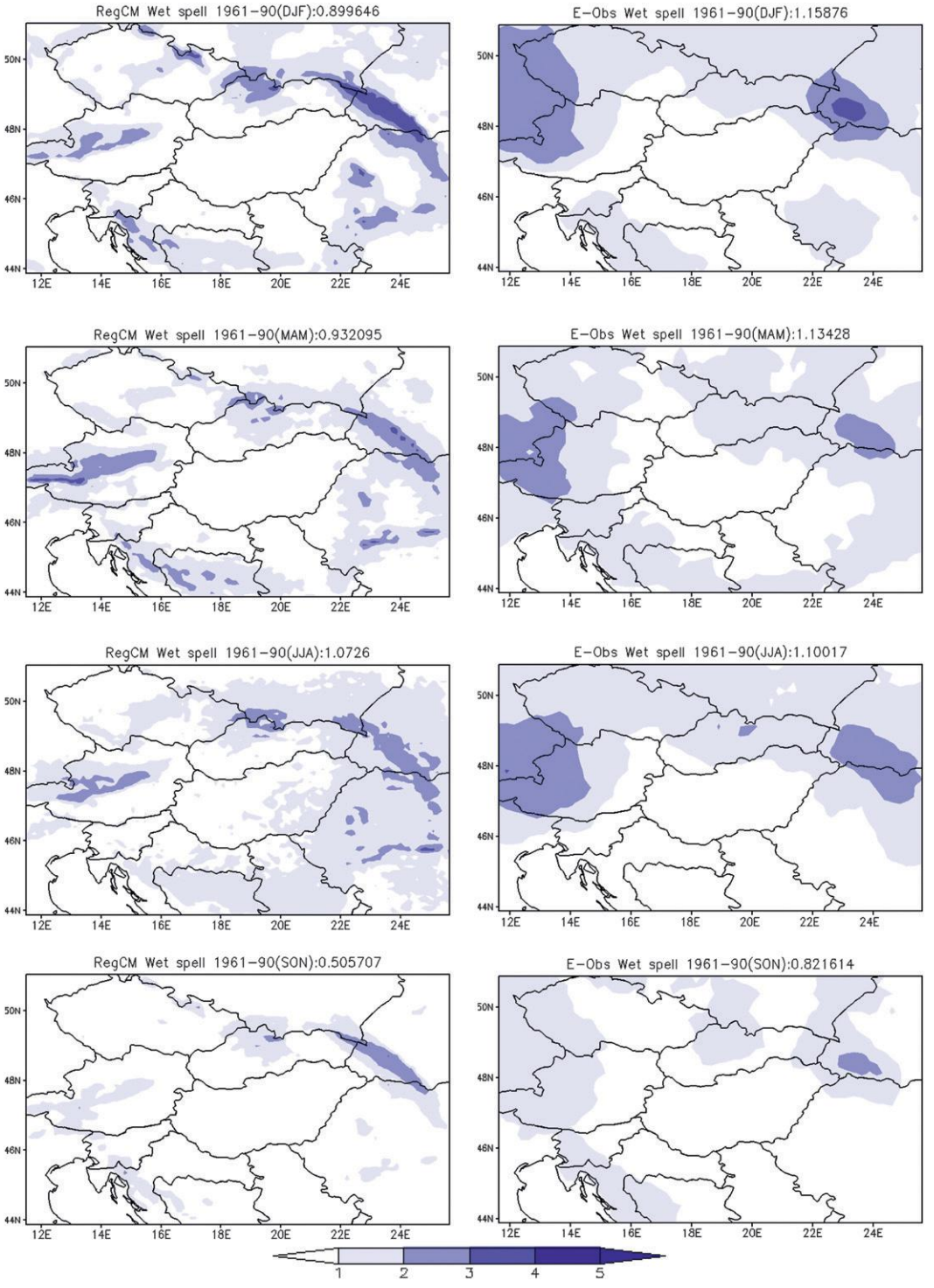

FIG. 14. As in Fig. 13, but for wet spell frequencies (refer to text).

a systematic underestimation of occurrences of wet spells can also be seen over the northwestern and northernmost parts of the integration domain. Concerning spatial distribution, the frequency of wet spells is closely related to topography, being at a maximum over the Carpathian and Alps chains and minimum over the Hungarian lowlands. The model reproduces this topographically forced spatial pattern, and in fact it produces a spatial detail that is more

refined than in the observed dataset. High-resolution observations would be needed to verify whether the additional spatial detail produced by the model is realistic. Overall, despite its positive precipitation bias, the model reproduces reasonably well the magnitude and spatial distribution of dry and wet spells.

5. Conclusions

We presented an assessment of a high-resolution version (10-km grid spacing) of the RegCM3 for the period 1961–90 over the Carpathian basin, with emphasis on the Hungarian territory. It is important to note that the grid spacing of 10 km is close to the limit of applicability of hydrostatic models, and therefore the model convection scheme and its interaction with the large-scale precipitation operates at its limits. We evaluated the model at a wide range of spatial and temporal scales, from the inner domain average to the grid point and local level, and from decadal to interannual and daily temporal scales.

The model reproduces the basic features of observed surface air temperature, from climatology to interannual and decadal scales. The main temperature systematic bias is an overestimation of January minimum temperatures. Overall, the seasonal temperature biases are less than 1°C, except in winter, when the bias can reach 2°C. The model tends to overestimate precipitation, especially in the cold season. This overestimation, however, is artificially enhanced by the lack of a rain gauge correction in the observations dataset, which may be up to 20%–30% in winter. The model reproduces well the observed interannual variability of temperature, except in winter, when this is underestimated. Interannual variability of precipitation is well reproduced, as is the frequency of dry and wet spells. The validation against two station datasets indicates that the model performance is not substantially degraded when going to the local scale, except for extreme summer precipitation events, which occur at convective, submodel grid scales.

This being the first multidecadal simulation of the RegCM3 at a grid spacing of 10 km, our results provide an encouraging indication of the use of a high-resolution version of this model, at least for extratropical regions. We assess that the model can provide useful information on variables that are important for the assessment of climate change impacts. We therefore plan to use this model configuration in simulations of future climate scenarios under increased greenhouse gas concentrations.

Acknowledgments. This paper was supported by the CECILIA project of the European Union No. 6 program (Contract GOCE-037005) and TÁMOP (Contract 4.2.1.B-09/1/KMR-2010-0005). We also acknowledge the E-Obs dataset from the EU-FP6 project ENSEMBLES (available online at http://www.ensembles-eu.org).

REFERENCES

Adam, J. C., and D. P. Lettenmaier, 2003: Adjustment of global gridded precipitation for systematic bias. *J. Geophys. Res.,* **108,** 4257, doi:10.1029/2002JD002499.

Christensen, J. H., and O. B. Christensen, 2007: A summary of the PRUDENCE model projections of changes in European climate during this century. *Climatic Change,* **81,** 7–30.

Csima, G., and A. Horányi, 2008: Validation of the ALADIN-Climate regional climate model at the Hungarian Meteorological Service. *Időjárás,* **112,** 155–177.

Déqué, M., and Coauthors, 2007: An intercomparison of regional climate simulations for Europe: Assessing uncertainties in model projections. *Climatic Change,* **81,** 53–70.

Dickinson, R., A. Henderson-Sellers, and P. Kennedy, 1993: Biosphere-Atmosphere Transfer Scheme (BATS) version 1 as coupled to the NCAR community climate model. NCAR Tech. Note NCAR/TN-387+STR, 72 pp.

Gao, X., J. S. Pal, and F. Giorgi, 2006: Projected changes in mean and extreme precipitation over the Mediterranean region from high resolution double nested RCM simulations. *Geophys. Res. Lett.,* **33,** L03706, doi:10.1029/2005GL024954.

Giorgi, F., 2006: Climate change hot-spots. *Geophys. Res. Lett.,* **33,** L08707, doi:10.1029/2006GL025734.

——, and L. O. Mearns, 1999: Introduction to special section: Regional climate modeling revisited. *J. Geophys. Res.,* **104,** 6335–6352.

——, and E. Coppola, 2007: European climate-change oscillation (ECO). *Geophys. Res. Lett.,* **34,** L21703, doi:10.1029/2007GL031223.

——, M. R. Marinucci, and G. T. Bates, 1993a: Development of a second-generation regional climate model (RegCM2). Part I: Boundary-layer and radiative transfer processes. *Mon. Wea. Rev.,* **121,** 2794–2813.

——, ——, ——, and G. De Canio, 1993b: Development of a second-generation regional climate model (RegCM2). Part II: Convective processes and assimilation of lateral boundary conditions. *Mon. Wea. Rev.,* **121,** 2814–2832.

Grell, G., 1993: Prognostic evaluation of assumptions used by cumulus parameterizations. *Mon. Wea. Rev.,* **121,** 764–787.

——, J. Dudhia, and D. R. Stauffer, 1994: A description of the fifth-generation Penn State/NCAR Mesoscale Model (MM5). NCAR Tech. Note NCAR/TN-398+STR, 121 pp.

Halenka, T., 2007: On the assessment of climate change impacts in central and eastern Europe - EC FP6 Project CECILIA. *Geophys. Res. Abstr.,* **9,** 10545. [Available online at http://meetings.copernicus.org/www.cosis.net/abstracts/EGU2007/10545/EGU2007-J-10545.pdf.]

Haylock, M. R., N. Hofstra, A. M. G. Klein Tank, E. J. Klok, P. D. Jones, and M. New, 2008: A European daily high-resolution gridded data set of surface temperature and precipitation for 1950–2006. *J. Geophys. Res.,* **113,** D20119, doi:10.1029/2008JD010201.

Hofstra, N., M. Haylock, M. New, and P. D. Jones, 2009: Testing E-OBS European high-resolution gridded data set of daily precipitation and surface temperature. *J. Geophys. Res.,* **114,** D21101, doi:10.1029/2009JD011799.

Holtslag, A. A. M., E. I. F. de Bruijn, and H.-L. Pan, 1990: A high resolution air mass transformation model for short-range weather forecasting. *Mon. Wea. Rev.,* **118,** 1561–1575.

Jacob, D., and Coauthors, 2007: An inter-comparison of regional climate models for Europe: Model performance in present-day climate. *Climatic Change,* **81,** 21–53.

Kiehl, J., J. Hack, G. B. Bonan, B. Boville, B. Briegleb, D. Williamson, and P. Rasch, 1996: Description of NCAR community climate model (CCM3). NCAR Tech. Note NCAR/TN-420+STR, 152 pp.

Marinucci, M. R., F. Giorgi, M. Beniston, M. Wild, P. Tschuck, A. Ohmura, and A. Bernasconi, 1995: High resolution simulations of January and July climate over the western Alpine region with a nested regional climate modeling system. *Theor. Appl. Climatol.,* **51,** 119–138.

Mitchell, T. D., T. R. Carter, P. D. Jones, M. Hulme, and M. New, 2004: A comprehensive set of high-resolution grids of monthly climate for Europe and the globe: The observed record (1901–2000) and 16 scenarios (2001–2100). Tyndall Centre Working Paper 55, 30 pp.

Pal, J. S., E. Small, and E. Elthair, 2000: Simulation of regional scale water and energy budgets: Representation of subgrid cloud and precipitation processes within RegCM. *J. Geophys. Res.,* **105,** 567–594.

——, and Coauthors, 2007: Regional climate modeling for the developing world: The ICTP RegCM3 and RegCNET. *Bull. Amer. Meteor. Soc.,* **88,** 1395–1409.

Pardo, E., S. Marín, V. Sanchis, and A. J. Ramos, 2005: Impact of relative humidity and temperature on visible fungal growth and OTA production of ochratoxigenic *Aspergillus ochraceus* isolates on grapes. *Food Microbiol.,* **22,** 383–389.

Räisänen, J., 2002: CO_2-induced changes in interannual temperature and precipitation variability in 19 CMIP2 experiments. *J. Climate,* **15,** 2395–2411.

Sansom, J., and A. J. Renwick, 2007: Climate change scenarios for New Zealand rainfall. *J. Appl. Meteor. Climatol.,* **46,** 573–590.

Solomon, S., D. Qin, M. Manning, M. Marquis, K. Averyt, M. M. B. Tignor, H. L. Miller Jr., and Z. Chen, Eds., 2007: *Climate Change 2007: The Physical Science Basis*. Cambridge University Press, 996 pp.

Torma, C., J. Bartholy, R. Pongracz, Z. Barcza, E. Coppola, and F. Giorgi, 2008: Adaptation and validation of the RegCM3 climate model for the Carpathian basin. *Időjárás,* **112,** 233–247.

Uppala, S. M., and Coauthors, 2005: The ERA-40 Re-Analysis. *Quart. J. Roy. Meteor. Soc.,* **131,** 2961–3012.